Energy Conversion and Management 266 (2022) 115835

Contents lists available at ScienceDirect

Energy Conversion and Management

journal homepage: www.elsevier.com/locate/enconman

Technology selection for capturing CO_2 from wood pyrolysis

Yingying Sun [a], Beibei Dong [a,b], Liang Wang [c], Hailong Li [b,*], Eva Thorin [b]

[a] Tianjin University of Commerce, China
[b] School of Business, Society and Technology, Mälardalens University, Sweden
[c] SINTEF Energy Research, P.O. Box 4761, Sluppen, 7465 Trondheim, Norway

ARTICLE INFO

Keywords:
Bioenergy with carbon capture and storage (BECCS)
Negative emission technologies
Pyrolysis
Economic analysis
Energy efficiency
Levelized cost of CO_2

ABSTRACT

Emerging negative emission technologies (NETs) are considered as effective measures to reduce carbon dioxide emissions to achieve the climate goal set by the Paris Agreement, and bioenergy with carbon capture and storage (BECCS) is one of the most important NETs. Integrating CO_2 capture with biomass pyrolysis (PyrCC) is attracting increasing interest, because biomass pyrolysis has been widely used to produce biooil to replace fossil fuel for decarbonizing the transport sector. In order to provide guidance to the selection of CO_2 capture technologies, this paper evaluated the technical and economic performances of PyrCC when different CO_2 capture technologies are integrated, including monoethanolamine-based chemical absorption (MEA-CA), temperature swing absorption (TSA), calcium looping (CaL), and chemical looping combustion (CLC). Generally speaking, CLC can realize the highest capture amount of CO_2 with the lowest energy penalty. Meanwhile, CLC and CaL show the lowest levelized cost of CO_2 (LCOC), which are around 56$/t$CO_2$; and on the contrary MEA-CA shows the highest one of 83 $/t$CO_2$. In addition, the key process parameter of pyrolysis, reaction time, has clear effects on the performance of CO_2 capture as the longer reaction time leads to an increased amount of captured CO_2 and reduced energy penalty. As a result, when the reaction time increases, the LCOCs of all assessed technologies decrease. Moreover, the net present value and the payback time are also estimated for different technologies. At the carbon price of 70.1$/t$CO_2$, MEA-CA and CLC show the longest and shortest payback time that are 5.9 years and 3.2 years respectively.

1. Introduction

According to the data observed by National Aeronautics and Space Administration (NASA) [1], the global temperature has risen by 2.1 °C since 1880; and 2016 and 2020 are tied together as the warmest years. According to the Paris Agreement [2], the contracting countries need to take effective measures to reduce greenhouse gas emissions, in order to control the global temperature rise below 2 °C above pre-industrial levels by 2050. To achieve such a goal, the report of the United Nations Environment Programme (UNEP) highlights that the annual CO_2 emissions in 2030 need to be reduced by 15 billion tons from the current level [3]. The emerging negative emission technologies (NETs), which can remove CO_2 directly from the air, have been considered as effective measures to reduce CO_2 emission. The Intergovernmental Panel on Climate Change (IPCC) report states if NETs can be widely deployed by the end of the century, the goal of the Paris Agreement is possible to be achieved [4]; otherwise, the probability of reaching the 1.5 °C target is less than 50% [5].

Bioenergy with carbon capture and storage (BECCS) is one of the most important NETs, which combines CO_2 capture and storage (CCS) with energy conversion and utilization of biomass. In general, the CO_2 capture technologies developed for fossil fuel can be adopted to bioenergy depending on their applicability. According to the report from Global CCS institute in 2019, there were 18 BECCS projects globally, mainly distributed in the North America, and Europe, with 5 already in operation [6]. CO_2 capture can be integrated with different biomass conversion and utilization processes, such as with pyrolysis plants in Norway and Netherland, with ethanol production plants in France, Brazil and Sweden, with biomass combustion plants in Japan, with two paper mills in Sweden, with a biomass gasification plant in the USA, and with a biogas plant in Sweden [7–9].

To realize decarbonization of the transport sector, different measures have been proposed and developed, one of which is to replace fossil oil with biooil produced from pyrolysis of biomass. Biomass pyrolysis is a thermochemical conversion process to heat biomass in an oxygen-starved atmosphere and crack it to solid, liquid and gaseous products.

* Corresponding author.
E-mail address: hailong.li@mdu.se (H. Li).

https://doi.org/10.1016/j.enconman.2022.115835
Received 1 April 2022; Received in revised form 13 May 2022; Accepted 29 May 2022
Available online 7 June 2022

The yield of liquid (biooil) can reach up to 70–75 wt% on dry biomass basis [10]. After upgrading by hydrodeoxygenation, hydrocracking, emulsification, steam reforming and esterification, it can be used as vehicle fuel [11]. With the development of biomass pyrolysis technologies, integrating CCS with pyrolysis is attracting more attention for achieving negative CO_2 emission. The produced syngas in pyrolysis is normally combusted in a separate burner to provide heat needed by pyrolysis. Compared to biomass combustion, the flue gas (FG) of syngas combustion contains higher volume concentrations of CO_2 (CO_2vol%). For example, for the pyrolysis of wood at 500 °C with reaction time less than 10 min, CO_2vol% in the FG is 16%~19 vol% [12,13]. The higher concentration of CO_2 can favor CO_2 capture. However, studies about the integration of CO_2 capture with biomass pyrolysis (PyrCC) are rare. Woolf et al. [14] compared the economic feasibility for the integration of CO_2 capture with both slow and fast pyrolysis in a general way; whereas, no concrete capture technology was considered. It was found that the integration with slow pyrolysis was more feasible due to the higher benefit from biochar; while if the price of biooil increased, fast pyrolysis may be more beneficial when taking into account the produced biooil. Lotte et al. [15] estimated the CO_2 reduction potential of different pathways in Denmark, including integrating CCS with pyrolysis. The general analysis without considering the detailed capture technology showed that it can contribute to a reduction of 2 $MtCO_2$ by 2030. Theodore et al. [16] conducted techno-economic analysis regarding the integration of CCS with switchgrass pyrolysis. The results showed that when the price of carbon was \$116/tCO_2, biooil produced from pyrolysis with CCS can be competitive with fossil oil. However, no capture technology was specified either. Schmidt et al. [17] assessed the economic performance regarding integrating chemical looping combustion (CLC) with pyrolysis. Results showed that CLC can potentially reduce the cost of CO_2 capture. However, there was no discussion on potential CO_2 capture. Cheng et al. [18] assessed the economic viability of biomass thermochemical conversion technologies combined with CCS, which included pyrolysis, hydrothermal treatment, gasification, and conventional combustion. It was found that the slow pyrolysis of wood combined with CCS had the best economic benefits. Nevertheless, there is no consideration about different capture technologies.

The main obstacle to the application of CO_2 capture is the high cost, although it has been significantly reduced from the 600\$/tonne, which was estimated by the American Physical Society in 2011, to 94–232 \$/tonne in 2018 [19]. The capture cost varies clearly with different capture technologies. To improve the economic feasibility of PyrCC and promote the development of PyrCC, selecting a proper capture technology is of great importance, which is mainly determined by the CO_2vol% in the FG. According to the possible CO_2vol%, the applicable capture technologies include monoethanolamine (MEA) based chemical absorption (MEA-CA) [20], temperature swing absorption (TSA) [21], calcium looping (CaL) [22] and chemical looping combustion (CLC) [23,24]. Here, pressure swing adsorption (PSA) is excluded because TSA was found more suitable according to the study of Bui et al. [25]. Even though there are many studies comparing different capture technologies, for example: Gardarsdottir et al. [26], Ho et al. [27], and Yang et al. [28], there has not been a comprehensive work that compares the capture technologies suitable for pyrolysis from both technical and economic perspectives. With the growing interest about integrating CO_2 capture with pyrolysis, a guideline for decision making on technology selection is of great significance.

In addition, biomass pyrolysis can generally be divided into slow and fast pyrolysis, mainly depending on the heating rate and reaction time. Fast pyrolysis is characterized with a high heating rate and short reaction time; while slow pyrolysis is a slow thermal degradation of the biomass with a low heating rate and long reaction time. The reaction time can considerably affect the yields and properties of pyrolysis products, and, consequently, affects the feasibility of PyrCC. Nevertheless, how the reaction time affects CO_2 capture remains unknown. In order to bridge the knowledge gap and provide guidance about the selection of CO_2 capture technologies, this work aims to compare the performance of PyrCC and investigate the cost of CO_2 capture under different pyrolysis time and by using different capture technologies.

2. Process description and simulation models

2.1. Pyrolysis integrated with CO_2 capture (PyrCC)

Fig. 1 shows the biomass pyrolysis with an external burner for combusting pyrolysis syngas. Biomass is heated in the reactor with absence or limited oxygen at different heating rates and temperatures [29], and the produced volatiles and gases further flow into a cooler. After cooling, the condensable gases are condensed and collected as biocrude; whereas the non-condensable syngas, which mainly consists of H_2, CO, and CH_4, is burnt in the burner to provide heat to the pyrolysis process. When CO_2 capture is integrated, it can be added after FG cleaning, which removes pollutants, such as NO_x. In this study, wood is chosen as raw material. Woody biomass is the currently most widely one used in pyrolysis plants with considering their attractive properties such as high energy density, large availability and low ash content [30–32]. Pyrolysis of woody biomass under dedicated conditions can achieve much better overall energy and climate change performances than other biomass feedstock [33].

The reaction time, which is counted from the moment the feedstock enters the reactor to the moment it leaves the reactor, has been identified as key operating parameter. It can also reflect the heating rate once the pyrolysis temperature is determined. In order to study the influence of reaction time, the kinetic model proposed by Ranzi et al. [34] was employed in the current work. The kinetic model was proposed and developed based on devolatilization of three main biomass components (cellulose, hemicellulose, and lignin) and used to predict yields of solid, liquid and gas products from pyrolysis. The decomposition and product formation upon reaction time can also be predicted by using the model, which were validated against experimental measurements. Based on the given kinetic parameters of the main reactions involved in pyrolysis, Peters et al. [35] implemented Ranzi's model in Aspen Plus, as shown in Fig. 2. Wood is first decomposed into cellulose, hemicellulose, and lignin in RDECOMP, which are further converted to biochar, biooil and syngas in CELLA, HCE and LIG respectively. RCSTR is used to model CELLA, HCE and LIG, in which the reactants, products, kinetic parameters of each reaction and reaction time are specified. More details about the Aspen Plus model, including the block information, can be found in Appendix A: Table A.1 and A.2. It is assumed that all products are completely separated and a complete combustion is achieved. The compositions of wood and biochar used in the simulation are listed in Table 1. The lower heating value of wood is 18.7 MJ/kg.

2.2. CO_2 capture technologies

Four different capture technologies, which are selected according to the applicability, are considered in this work, including monoethanolamine-based chemical absorption (MEA-CA), temperature swing absorption (TSA), calcium looping (CaL), chemical looping combustion (CLC).

2.2.1. MEA based chemical absorption (MEA-CA)

MEA-CA is one of the most developed CO_2 capture technologies and a general sketch of MEA-CA is shown in Fig. 3. In the absorber, the lean solution absorbent reacts with CO_2 to remove it from the FG. After absorption, the rich solution is sent to the stripper for solvent regeneration, in which CO_2 is released and the regenerated lean solution is recirculated. To reduce the heat demand of solvent regeneration, a heat exchanger is added to recover the heat from the regenerated lean solvent. To simulate such a process, a rate-based model [38] is developed in Aspen Plus with inputs summarized in Table 2.

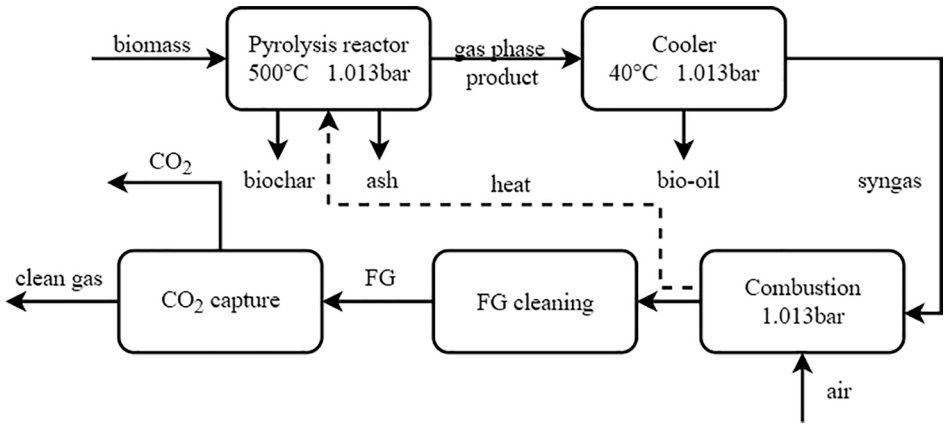

Fig. 1. Process scheme of pyrolysis integrated with CO_2 capture.

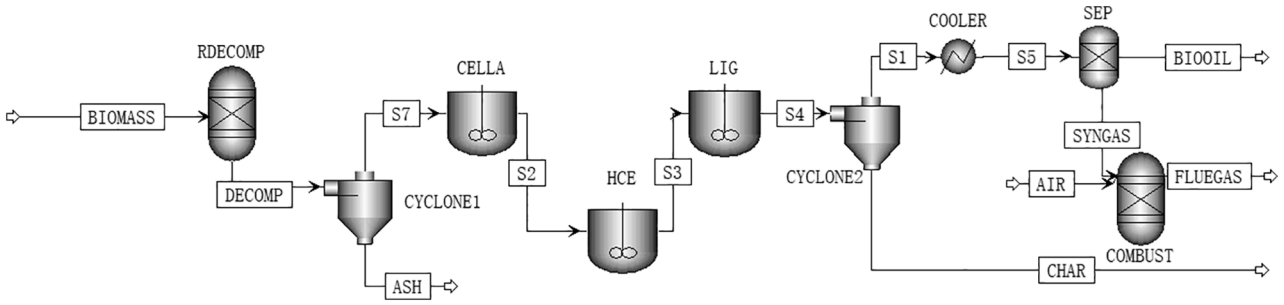

Fig. 2. Aspen Plus flowsheet of pyrolysis.

Table 1
Elemental and industrial analysis of biomass and biochar [36,37].

	Proximate Analysis (%, on dry basis)				Ultimate Analysis (%, ash free and on dry basis)				
	Moisture	Ash	Volatile matter	Fixed carbon	C	H	O	N	S
Wood	7.00	4.80	76.20	19.00	47.85	5.12	41.21	0.8	0.22
Biochar	0	11.40	44.11	44.49	77.33	3.20	17.37	0.68	1.42

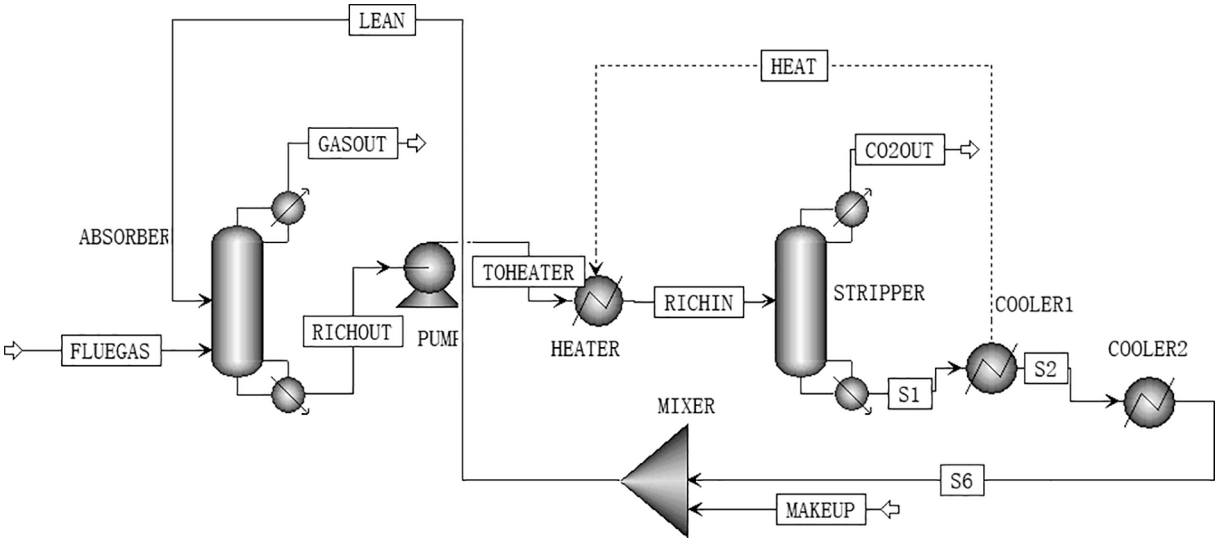

Fig. 3. Aspen Plus flowsheet of MEA-CA.

Table 2
Inputs of models for different capture technologies.

MEA-CA [38]			TSA [39]		CaL [43]		CLC [44]			
Inlet FG	T/°C	31.7	Desorption temperature (T_H)/°C	118	Carbonation/°C	650	Air reactor		Fuel reactor	
	P/bar	1.061	Adsorption temperature (T_L)/°C	48	Calcination/°C	900	T/°C	1150	T/°C	835
MEA concentration/wt %	28.30		High pressure (P_H)/bar	1×10^5	F_R/F_0	30	P/bar	17.53	P/bar	16.63
Lean loading/(mol/mol)	0.297		Heating temperature $(T_{hea})_t$/°C	128			Excess O_2/wt %	5.00	NiO/kg/s	480.54
Parameters	Adsorber	Stripper	Cooling temperature (T_{cool})/°C	38					$NiAl_2O_4$/ kg/s	135.46
Number of plates	20	20								
P/bar	1.061	1.819								
T/°C		117.8								

* F_R: adsorbent recirculation; F_0: adsorbent makeup.

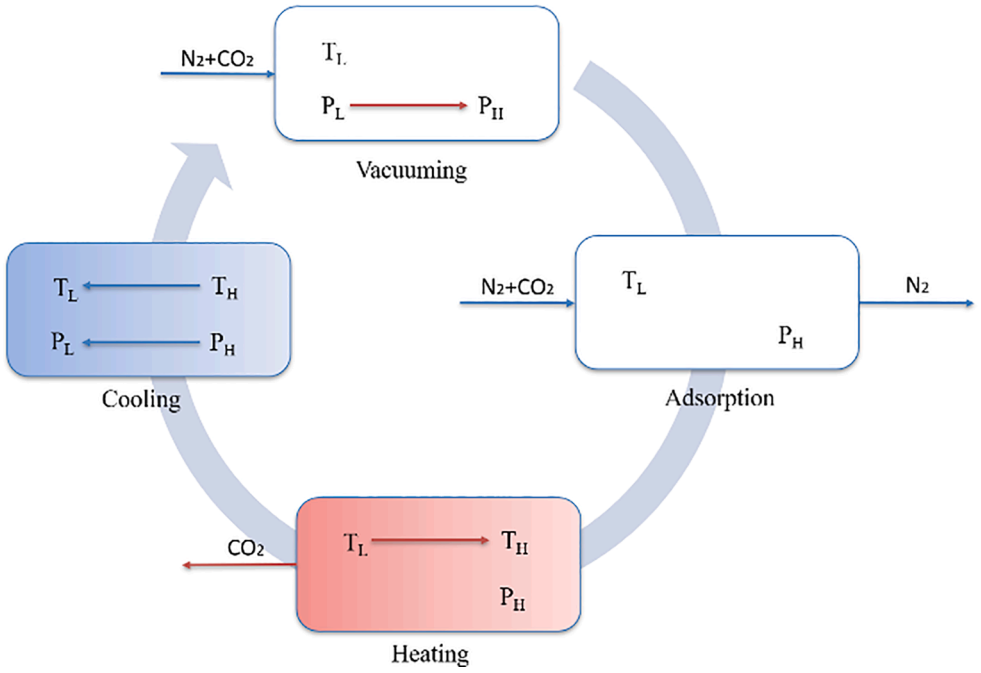

Fig. 4. Flowsheet of temperature swing absorption (TSA).

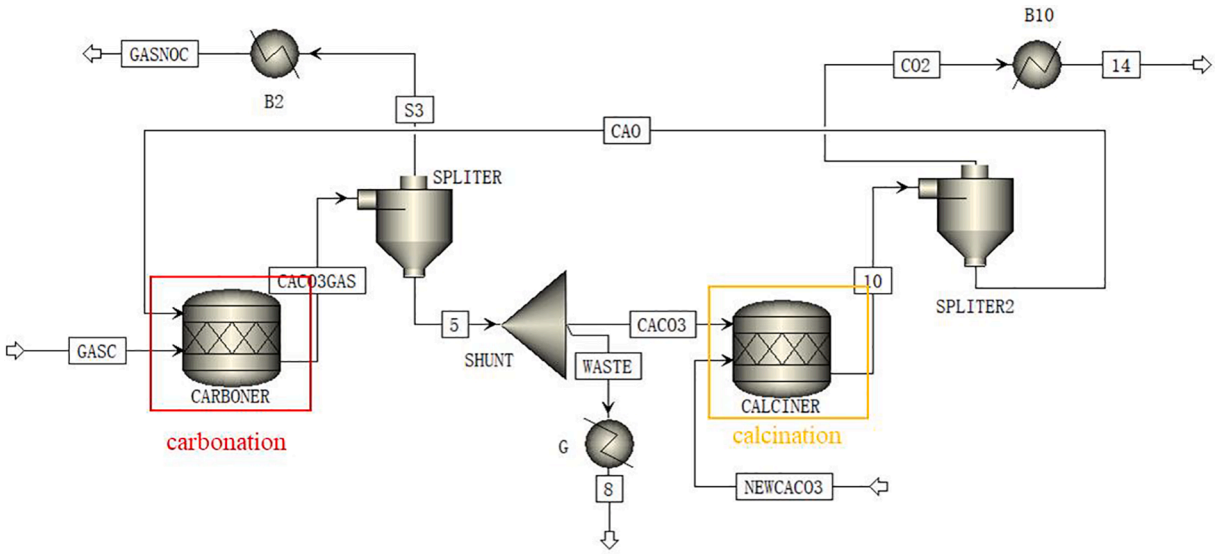

Fig. 5. Flow sheet of Calcium looping (CaL).

2.2.2. Temperature swing absorption (TSA)

The process of TSA can be divided into four steps, as shown in Fig. 4: (i) vacuumizing: the column filled with adsorbents is vacuumized before FG is fed from the bottom; (ii) adsorption: CO_2 in the FG is selectively adsorbed on the adsorbent, which is Zeolite 13X in this work; (iii) heating: the adsorbents are heated to T_H (118 °C) using heat transfer fluid to release CO_2; and (iv) cooling: the temperature of the reactor is cooled down to $T_L = 48$ °C before the next cycle begins. To simulate such a process, the model from Zhao et al. [39] is adopted, which is implemented in Matlab. The model details can be referred to [39] and the key inputs are also summarized in Table 2.

2.2.3. Calcium looping (CaL)

CaL is a promising CO_2 capture technology that may achieve a lower cost than MEA-CA [40]. The CaL technology (as shown in Fig. 5) is mainly composed of two steps, carbonation and calcination. The principle of separation can be described by Reaction (1). FG enters the carbonizer where CO_2 and CaO undergo an exothermic reaction at 650 °C to form $CaCO_3$; and $CaCO_3$ is separated and sent to the calciner to be decomposed into CaO and CO_2 at 900 °C. After calcination, CO_2 is released and CaO is recirculated. Zhang et al. [41] and Gao et al. [42] proposed to combine the carbonization of CaO with gasification, which can reduce CO_2 and energy consumption. But both did not include the calcination process. In addition, it is common to integrate CaL with fuel conversion to achieve in-situ capture, which can result in a lower energy consumption due to better heat transfer. However, this is not suitable for the integration with pyrolysis. Since biochar is considered as an important product and needs to be separated, adding CaO directly in the reactor will make biochar separation difficult. Therefore, pyrolysis and CO_2 capture are separated in this work. The CaL is modelled in Aspen Plus based on the work of Rolfe et al. [43]. The main inputs of the model are shown in Table 2.

$$CaO + CO_2 \rightleftharpoons CaCO_3 \quad \Delta H = \pm 179 kJ \bullet mol^{-1} \tag{1}$$

2.2.4. Chemical looping combustion (CLC)

The air combustion can be replaced by chemical looping combustion (CLC), as shown in Fig. 6, which belongs to oxy-fuel combustion capture. In the fuel reactor (FR), metal oxides react with hydrocarbons. Metal oxides are reduced to metal, and hydrocarbons are converted to CO_2 and H_2O. Since the oxidized gas mainly consists of CO_2 and H_2O, CO_2 can be separated after H_2O is condensed. The reduced metal is oxidized in the air reactor (AR) before the metal oxides are recirculated. In this work, $NiO/NiAl_2O_4$ is used as the oxygen carrier. The CLC model is also built in Aspen Plus, according to the work of Khan et al. [44], and the inputs are summarized in Table 2.

2.3. Model Validation

For model validation, the absolute relative deviation (ARD) is used, which is defined as follows:

$$ARD = \left| \frac{(x_{ref} - x_{xim})}{x_{ref}} \right| \times 100\% \tag{2}$$

where x_{ref} and x_{sim} are the reference value and simulated result of the key output used for model validation.

2.3.1. Pyrolysis model

To validate the pyrolysis model, the yields of gas, oil and char are compared with the experimental data from Ephraim et al. [45] and the simulation results from Shahbaz et al. [46]. As shown in Table 3, the biggest deviation is on char, which is 5.3%. In addition, since the gas composition of FG, especially CO_2vol%, can clearly impact the performance of CO_2 capture technology, the model is also validated through comparing the syngas composition. The simulation results from Visconti et al. [47] is employed and results are also presented in Table 3. It can be seen that the deviation on CO_2 is only 1.2%.

2.3.2. MEA-CA model

To validate the model of MEA-CA, the simulated results are compared with the experimental results of Li et al. [38], including rich solvent load, captured CO_2, reboiler temperature, reboiler load and CO_2 purity, as shown in Table 4. The deviations are all below 5%.

2.3.3. TSA model

To validate the model of TSA, the simulated results are compared with the simulated results of Zhao et al. [39] and the experimental data of Merel et al. [48]. As shown in Table 5, the deviations are all below 5%.

2.3.4. CaL model

The CaL model is validated by comparing the flow rate of captured CO_2, CO_2 capture rate and energy penalty of carbonator with the simulated results of Rolfe et al. [43], Vorrias et al. [49] and Ortiz et al. [50], and the experimental results of Arias et al. [50]. As shown in Table 6, a good agreement can be observed with ARD below 4%.

2.3.5. CLC model

The validation of the CLC model is shown in Table 7, in which our simulated results are compared with those simulated results from Khan et al. [44] on outlet composition of fuel reactor and air reactor. The flow rate of FG is 16.5 kg/s, and the mole fraction of CH_4 is 89%. The maximum deviation is about 7%.

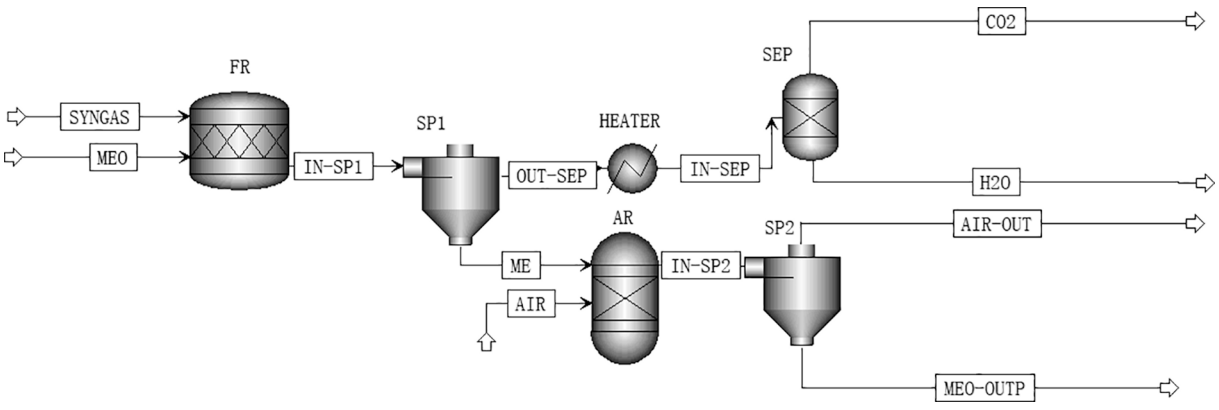

Fig. 6. Flow sheet of chemical looping combustion (CLC).

Table 3
Validation of the Pyrolysis model.

Input		[45] (exp)		[46] (sim)			[47] (sim)		
Feedstock		poplar wood		lignocellulosic biomass			lignocellulosic biomass		
T/°C		750		450			500		
P/bar		1.013		1			1		
Reaction time/min		0.5		30			20		
Output	[45] (exp)	This study	ARD /%	[46] (sim)	This study	ARD /%	[47] (sim)	This study	ARD /%
Gas/wt%	15.7	14.9	5.1	52	49.6	4.6			
Oil/wt%	63.7	63.5	0.3	26	24.9	4.2			
Char/wt%	20.6	21.6	4.9	22	25.5	5.3			
H_2/mol%							41	42.1	2.7
CO/mol%							5	4.8	4
CO_2/mol%							26	25.7	1.2
CH_4/mol%							17	17.9	5.2
H_2O/mol%							11	9.5	13.6

Table 4
Validation of the MEA-CC model.

Input		[38]			[38]			[38]	
T_{lean}/°C		39.4			33.9			32.4	
MEA% of lean/wt-%		28.3			31.6			33.5	
Lean loading/(mol/mol)		0.297			0.314			0.254	
FG flow rate/(kg/hr)		596.0			482.8			646.1	
CO_2 %		11.6			13.4			12.9	
Output	[38]	This study	ARD /%	[38]	This study	ARD /%	[38]	This study	ARD /%
Rich loading/(mol/mol)	0.512	0.506	1.2	0.481	0.511	6.2	0.494	0.508	2.8
Captured CO_2/(kg/h)	83.8	84.1	0.4	74.2	72.6	2.2	96.9	93.9	3.1
$T_{reboiler}$/°C	121.1	122.2	1.0	117.2	119.3	1.8	125.3	126.5	1.0
$Q_{reboiler}$/ (MJ/kgCO_2)	4.11	4.19	1.9	4.33	4.47	3.2	4.01	4.03	0.5
CO_2 purity/ (vol%)	99.1	99.0	0.1	97.6	97.4	0.2	98.9	98.4	0.5

Table 5
Validation of the TSA model.

Input		[39]			[39]			[48]	
CO_2/mol%		15			15			10	
T_H/°C		118			112			140	
T_L/°C		48			35			25	
Output	[39]	This study	ARD /%	[39]	This study	ARD /%	[48]	This study	ARD/ %
CO_2 purity/vol%	77.5	79.5	2.6	80	83.2	4	94	96.7	2.9
Energy penalty/ (MJ/kgCO_2)	7.2	6.9	4.2	6.3	6.0	4.8	8.8	8.56	2.7
W_{min}/(kJ/kgCO_2)	119	115	3.4	127	122	3.9			
Eff_{2nd}/%	5.7	5.5	3.5	8.5	8.2	3.5			
CO_2 capture rate/%							65	67.3	3.5

Table 6
Validation of the CaL model.

Input	[43]			[49]			[50]			[51]		
FG flow rate	291.6 kg/s			403.8 kg/s			699.25 kg/s			14.3 mol/s		
CO_2	94 wt-%			12.34 wt-%			20 wt-%			14 vol%		
F_R/F_0	40			70			20			60		
Output	[43]	This study	ARD /%	[49]	This study	ARD /%	[50]	This study	ARD /%	[51]	This study	ARD /%
Captured CO_2	274.1 kg/s	269.0 kg/s	1.9							2.0 mol/s	1.95 mol/s	2.3
$Q_{carbonator}$	1262.0 MW	1265.6 MW	0.3	303 MW	311.6 MW	2.8	711 MW	696.7 MW	2.0			
CO_2 capture rate				93.93%	97.32%	3.6	77%	77.6%	0.8	88%	87%	1.1

Table 7
Validation of the CLC model.

Input		Fuel reactor		Air reactor		
Excess O_2/wt%		5.00		NiO/kg/s		480.54
				$NiAl_2O_4$/ kg/s		135.46
Output (mol %)	[44]	This study	ARD/ %	[44]	This study	ARD/ %
CO_2	34.66	33.69	2.8	0.03	0.03	0
H_2O	65.06	66.01	1.5	1.08	1.08	0
N_2	0.28	0.30	7.1	82.40	82.43	0.04
O_2				15.61	15.58	0.2
Ar				0.88	0.88	0
Ni	54.65	54.97	0.6			
NiO	23.36	23.04	1.4	78.01	78.01	0
$NiAl_2O_4$	21.99	21.99	0	21.99	21.99	0

3. Performance of fast and slow pyrolysis of wood integrated with CO_2 capture

To assess the feasibility and performance of integrating CO_2 capture with pyrolysis, a real plant is chosen as a case study, which produces 25,000 tonne biooil per year with an operation time of 7500 hr/year [52]. The mass flow rate of wood is 21978 kg/h. The temperature and pressure of pyrolysis are 500 °C and 1 atm respectively. By using the validated models presented in Section 2, the performances of different capture technologies are compared, and the influences on the energy efficiency and costs of pyrolysis are investigated.

3.1. Studied cases

Pyrolysis process parameter such as temperature and reaction time can considerably affect the yield and properties of products, which can further influence the conversion efficiency of pyrolysis. Consequently, change of the amount and properties of gas products from pyrolysis at various conditions can also influence the performance of CO_2 capture. Temperature gives evident effects on yield of products from pyrolysis of biomass, especially the liquid and gaseous products [53]. For both fast and slow pyrolysis, the highest yield of liquid product is obtained in temperature range of 450–550 °C, while the gaseous product yields increase gently [54]. With the consideration of optimal production of biooil through pyrolysis, temperature of 500 °C is selected in the current work and attention is mainly focused on the effect of reaction time on gas yield and further CO_2 capture potential. Fig. 7 displays the variation of solid, liquid and gas yields with time. In general, as the reaction time increases, the share of solid, i.e., biochar, increases, while the share of bio-oil decreases clearly. On the contrary, the share of gas is not affected by time very much. Moreover, when the reaction time is over 10mins,

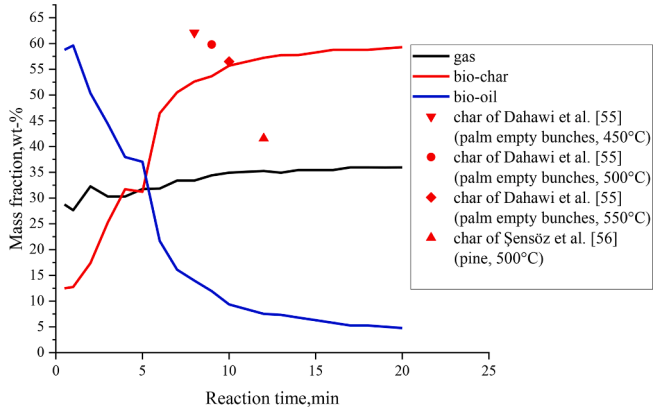

Fig. 7. Yields of gas, oil and char as a function of reaction time based on simulations.

the variation of the shares become negligible (less than 4%). Some results on biochar yield collected from the literature [55,56] are also added to verify the results are reasonable. In order to take into account the impacts of reaction time, four cases are considered in this work as shown in Table 8, which include three fast pyrolysis cases and one slow pyrolysis case. The compositions of FG for the four cases are also listed in Table 8, as they are needed as inputs for the simulation of CO_2 capture.

3.2. Performance comparison of different CO_2 capture technologies

To compare the performance of different CO_2 capture technologies, the purity of captured CO_2, the amount of captured CO_2, the energy penalty of CO_2 capture are used as key performance indicators (KPIs). In addition, different processes need different forms of energy and even for the same form, e.g., heat, the required temperature can also be different. Therefore, it is unfair to compare the energy penalty directly since the quality of the energy consumed by CO_2 capture is different. To fairly compare different capture technologies, exergy penalty is also introduced, which can be calculated as:

$$Exergy\ penalty = dE_h + dE_e \tag{3}$$

$$dE_h = Q^*(1 - \frac{T_C}{T_D}) \tag{4}$$

$$dE_e = electricity \tag{5}$$

where dE_h is the exergy of consumed heat, in MJ/tCO_2, T_C is the ambient temperature, 293 K, T_D is the temperature of needed heat, in K, and dE_e is the exergy of consumed electricity, in MJ/tCO_2.

Fig. 8(a) shows the purity of captured CO_2. Both MEA-CA and CaL can achieve a high purity of captured CO_2 about 99.9 vol%. N_2 is the main impurity in the captured CO_2, when CLC and TSA are used. For TSA, multi-stage adsorption or a downstream CO_2 conditioning process are needed to further increase the purity depending on the requirement of CO_2 transportation and storage. Fig. 8(b) shows the flowrate of captured CO_2 when the reaction time changes. Generally speaking, the yield of syngas increases with the increase of reaction time, and therefore, it is possible to capture more CO_2. There is no problem to capture all CO_2, however, pursuing a high capture rate may increase the energy penalty. In this work, a capture rate of 90% is assumed for MEA-CA, TSA and CaL. Since TSA has the lowest CO_2 purity, the flowrate of captured CO_2 is higher than those from MEA-CA and CaL for the same CO_2 capture rate. For oxyfuel combustion capture technologies, such as CLC, normally all CO_2 is captured. Therefore, as illustrated in Fig. 8(b), CLC shows the highest capture amount. Fig. 8(c) shows the changes of energy penalty due to CO_2 capture. The increase of reaction time can result in higher CO_2vol% in the FG, which favors both the chemical absorption and physical adsorption, i.e., MEA-CA and TSA. Nevertheless, the change of CO_2vol% doesn't affect CaL clearly. For CaL, the energy penalty is mainly determined by the ratio of the adsorbent recirculation to the makeup (F_R/F_0) [50]. This study assumed a constant ratio, which is 30, so the change in energy penalty is not obvious. Comparing the energy penalty of all studied capture technologies shows that CLC consumes the least, which is followed by TSA, MEA-CA and CaL. Fig. 8(d) shows the changes of exergy penalty, which varies in similar ways to the energy penalty. CLC and CaL still consume the least and most exergy correspondingly. However, the differences between CLC, TSA and MEA-CC are much smaller, mainly due to the low temperature needed for regeneration.

3.3. Performance of pyrolysis integrated with CO_2 capture

To assess the influence of CO_2 capture on the performance of pyrolysis, the energy efficiency was employed as KPI, which is defined as:

Table 8
Pyrolysis condition, yields and composition of the produced gas of studied cases.

Cases	Reaction time	Shares of products			Gas composition/vol%			
		Char/wt%	Biooil/ wt%	Gas/wt%	CO_2	H_2O	O_2	N_2
FP1	30s	12.49	58.76	28.75	15.93	13.51	4.59	65.97
FP2	3 min	25.28	44.41	30.31	16.59	16.72	4.59	62.10
FP3	5min	31.21	37.04	31.75	17.24	19.87	4.59	58.30
SP1	10min	55.7	9.37	34.93	18.50	26.03	4.59	50.88

* FP: fast pyrolysis; SP: slow pyrolysis.

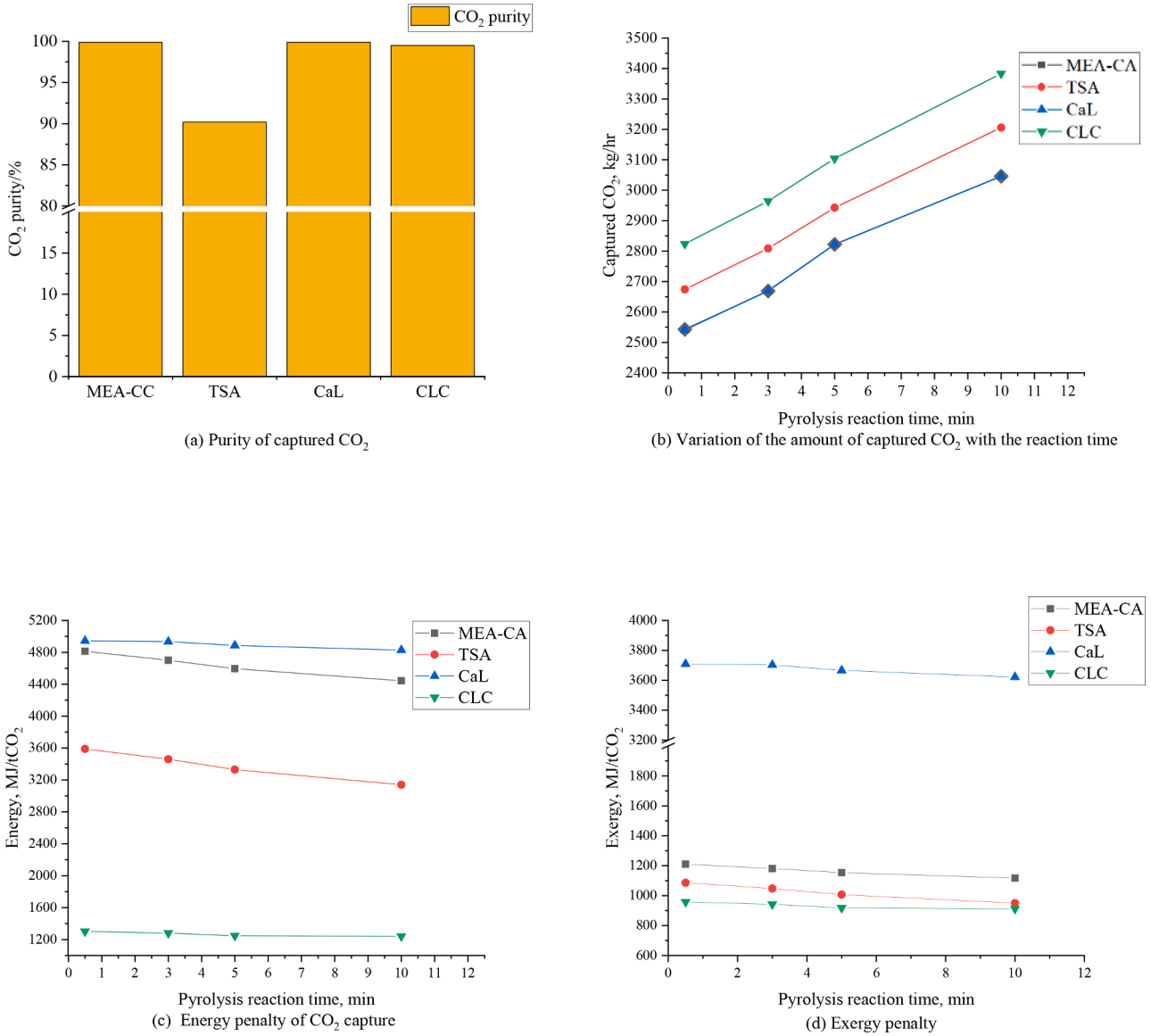

(a) Purity of captured CO_2

(b) Variation of the amount of captured CO_2 with the reaction time

(c) Energy penalty of CO_2 capture

(d) Exergy penalty

Fig. 8. The performance of CO_2 capture. (a) Purity of captured CO_2, (b) Variation of the amount of captured CO_2 with the reaction time, (c) Energy penalty of CO_2 capture and (d) Exergy penalty of CO_2 capture.

$$Energy\ efficiency = \frac{Output\ energy}{Input\ energy}\% \quad (6)$$

where *Output energy* includes the calorific value of all pyrolysis products, i.e., liquid and solid, and *Input energy* includes the supplied heat and the calorific value of the feedstock.

This study assumes that syngas is burned to generate heat. However, as CO_2 capture is integrated, it is not enough to cover the heat needed by both pyrolysis and CO_2 capture. Therefore, extra biomass, same as pyrolysis feedstock, is combusted to fill in the gap of heat demand.

Table 9 shows the energy efficiency of different cases without and with CO_2 capture. It is obvious that the efficiency of the pyrolysis system decreases as the reaction time increases, and the energy efficiency decreases when the capture technology is included. As the reaction time increases, the effect of CO_2 capture on the energy efficiency of the system gradually decreases. Different capture technologies have different effects on the energy efficiency of PyrCC. The least impact is from CLC, followed by TSA; while CaL has the greatest impact.

Fig. 9 shows the additional feedstock required when different CO_2

Table 9
Energy efficiency for different pyrolysis integrated with different CO_2 capture technologies.

Case	Parameters	FP1	FP2	FP3	SP4
Pyrolysis without CO_2 capture	FG flowrate/(kg/hr)	6319	6662	6978	7677
	CO_2% of FG/(vol%)	16	17	17	19
	Energy efficiency	94%	87%	83%	69%
Pyrolysis + MEA-CA	Captured CO_2/(kg/hr)	2541	2670	2822	3046
	Energy penalty/(MJ/tCO_2)	4814	4701	4595	4445
	Energy efficiency	81%	74%	71%	59%
Pyrolysis + TSA	Captured CO_2/(kg/hr)	2674	2809	2942	3206
	Energy penalty/(MJ/tCO_2)	3590	3460	3330	3140
	Energy efficiency	84%	77%	73%	61%
Pyrolysis + CaL	Captured CO_2/(kg/hr)	2541	2670	2822	3046
	Energy penalty/(MJ/tCO_2)	4944	4935	4886	4828
	Energy efficiency	77%	71%	68%	56%
Pyrolysis + CLC	Captured CO_2/(kg/hr)	2824	2964	3104	3383
	Energy penalty/(MJ/tCO_2)	1303	1281	1247	1241
	Energy efficiency	87%	80%	76%	63%

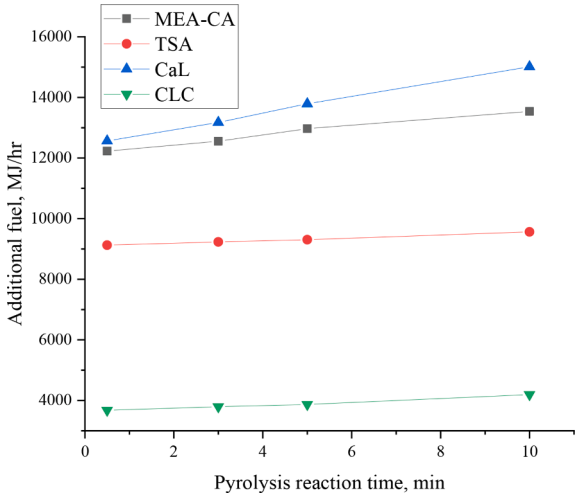

Fig. 9. Variation of the need of additional feedstock due to CO_2 capture with reaction time.

capture technologies are adopted. In general, it varies in the same way as the energy penalty of different technologies (as shown in Fig. 8(c)). In addition, as the reaction time increases, the amount of captured CO_2 increases and consequently more heat is needed. The impact of reaction time on the additional heat is most obvious for CaL, due to the constant F_R/F_0, which shall be optimized for different CO_2 amounts.

4. Influence of CO_2 capture on costs

4.1. KPIs

To compare the economic feasibility for different CO_2 capture technologies, only the cost associated with CO_2 capture is considered. Levelized cost of CO_2 (LCOC), net present value (*NPV*) and payback time (*PBT*) are chosen as the key performance indicators (KPIs) for evaluation purpose.

LCOC is a common KPI to evaluate the cost of CO_2 capture, which presents the cost over the life cycle of CO_2 capture equipment. It is calculated by using Eq (7).

$$LCOC = \frac{(CAPEX \bullet (1+i)^n + OPEX \bullet n)}{total\ amount\ of\ captured\ CO_2} \tag{7}$$

where *CAPEX* is the total investment cost ($), *OPEX* is the annual operating cost ($), n is the life of the capture plant (year), which is assumed to be $n = 20$; and i is the annual discount rate, $i = 8\%$ [57].

NPV and PBT are also commonly used to reflect the project profitability. If the achieved negative emission can be traded in the carbon market, profits can be made. NPV and PBT are defined by Eq (8) and (9) respectively.

$$NPV = \sum_{t=0}^{n} (CI - OPEX)_t (1+i)^{-t} \tag{8}$$

$$PBT = \frac{CAPEX}{(CI - OPEX)} \tag{9}$$

$$CI = CO_2\ price \times annual\ captured\ CO_2 \tag{10}$$

where *CI* is the profit from carbon trading, t is the t-th year in the lifetime, and *CAPEX* is total capital cost.

CAPEX mainly includes equipment cost and installation cost. The size of equipment is determined based on the simulation results. The six-tenths rule [58] is used to estimate the equipment costs when the system size varies. To consider the influence of time, e.g., inflation, the chemical engineering plant cost index (CEPCI) [59] is adopted to convert all costs to 2021. *OPEX* includes labor cost, maintenance cost and other costs related to materials consumption (such as chemicals, cooling water and electricity) in the operation, which is assumed proportional to *CAPEX*. The details of *CAPEX* and *OPEX* can be found in the Appendix B: Table B.1-4.

4.2. LCOC

Fig. 10 compares the LCOC of different capture technologies. In general, with the increase of the reaction time, the LCOC of each capture technology decreases slightly. From FP1 to SP4, the biggest change comes from CaL, which is 8.0%. MEA-CA shows the highest LCOC for all assessed cases. Compared to other technologies, the OPEX cost of MEA-CA has the biggest share due to its high energy penalty. CLC and CaL have very close LCOCs, which are the lowest. CLC and CaL also have similar OPEX. Even though the absorber used by CaL is cheaper, more labor work is needed to pretreat and change adsorbents, which deactivate quickly [60]. Moreover, TSA has the highest CAPEX cost, which is due to the high cost of the CO_2 adsorption column.

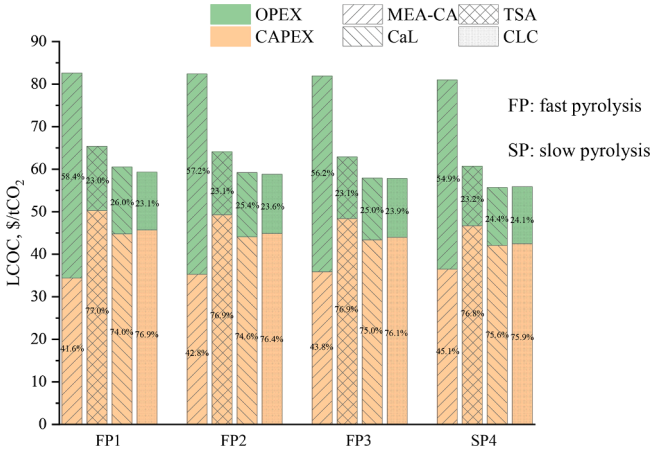

Fig. 10. LCOC of PyrCC integrated with different capture technologies.

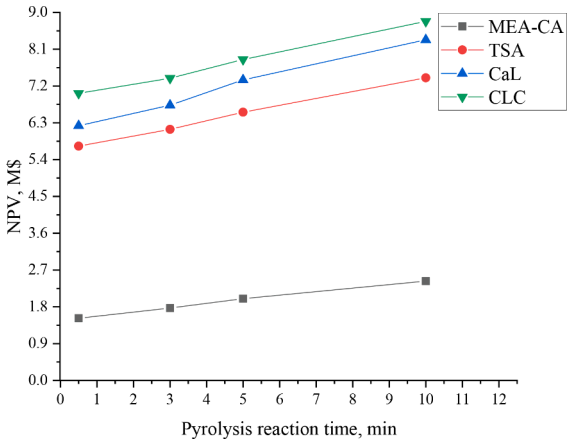

Fig. 11. Variation of NPV of PyrCC with reaction time.

4.3. NPV and PBT

To estimate NPV and PBT, the price of CO_2 is taken from EU Carbon Exchange data in December 2021 [61], which is 70.1$/t$CO_2$.

Fig. 11 shows the variation of NPV for different technologies. CLC shows the highest NPV in all studied cases because it has the lowest capture cost and captures the most CO_2, which further leads to the highest profit. On the contrary, MEA-CA has the lowest NPV, mainly due to its highest capture cost. For all capture technologies, with the increase of reaction time, as more CO_2 can be captured, the profit from carbon credit increases, and in consequence, NPV rises.

Fig. 12 shows the variation of PBT. As the carbon price has a significant influence on the economics of CO_2 capture integration, a sensitivity study is carried out. Naturally, PBT decreases with the increase of the carbon price. In particular, the change of the carbon price has the most significant effect on PBT of MEA-CA in comparison to others. The PBT of MEA-CA drops from 20.5 years to 4.1 years when the price increases from 40$/t$CO_2$ to 85$/t$CO_2$. On the contrary, the PBT of CLC and CaL are affected much less. Moreover, the PBT is not clearly affected by the reaction time. The variation is usually less than 3 years from FP1 to SP4.

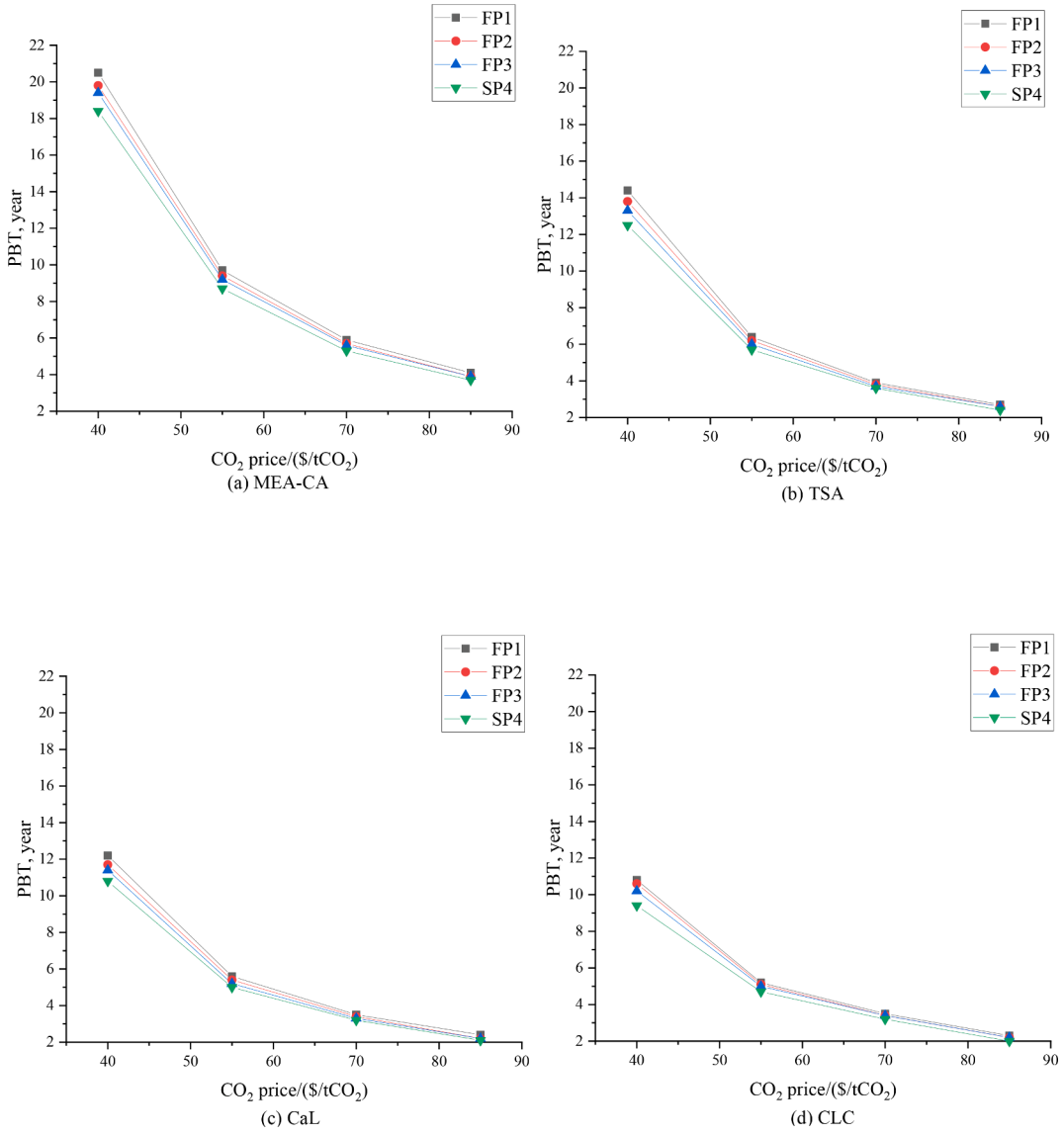

Fig. 12. Variation of PBT with CO_2 price for different capture technologies.

4.4. Discussions

Compared with MEA-CA and TSA, CaL and CLC are less mature [17,25]. Even though there are pilot tests, they haven't been tested in large scales, which implies there could be a big potential for cost reduction in the future. In addition, the integration of CO_2 capture is not optimized. For example, for CaL, CO_2 capture is separated from pyrolysis, which can potentially influence the heat integration and heat transfer, and lead to a lower energy efficiency. So it is suggested in the future work that more efforts shall be dedicated to the optimization regarding the integration of CO_2 capture with pyrolysis.

The scale of the capture equipment will also have a clear impact on the cost of CO_2 capture. Under the same CO_2 concentration, a larger-scale capture system can achieve a lower LCOC. In this study, the simple six-tenths rule is adopted, which can also result in uncertainties.

It is also worth to point out that in this study, only the pyrolysis in an environment of N_2 is considered due to the availability of data for model development and validation. However, it is also interesting to investigate the pyrolysis in other gas environments, such as CO_2 environment. It will change the composition of pyrolysis syngas and CO_2vol% of the gas stream going into CO_2 capture. Meanwhile, only woody biomass is selected as the raw feedstock for pyrolysis. Other types of biomass can also be pyrolyzed, which can lead to changes in the yield of syngas, and consequently changes in CO_2vol% of FG. The variation of CO_2vol% can further affect the energy consumption and cost for integrating CO_2 capture with pyrolysis. Even though the potential influences of CO_2vol% have been analyzed, further investigation is still suggested to obtaining more precise results for decision making. In addition, the operating temperature of pyrolysis also varies, depending on pyrolysis technologies and properties of biomass. More systematic studies are suggested to evaluating such effects of pyrolysis temperature on product distribution and further the energy efficiency and economics for the integration of CO_2 capture. Moreover, the impacts of reaction time on the yields at different operation temperatures also need to be understood more deeply.

5. Conclusions

This paper performs a technical and economic analysis for integrating CO_2 capture with pyrolysis in order to achieve negative emissions. 4 capture technologies are included, including MEA based chemical absorption (MEA-CA), temperature swing absorption (TSA), calcium looping (CaL) and chemical looping combustion (CLC). Based on simulations on wood pyrolysis in N_2, the following conclusions are drawn:

Technically, CLC is found to be superior to others due to its highest CO_2 capture rate with the lowest energy and exergy penalty; while CaL has the highest energy and exergy penalty.

The pyrolysis reaction time shows clear impacts on the potential of capture CO_2. With increase of time, more CO_2 can be captured with lower energy penalty for all studied capture technologies.

The integration of CO_2 capture with pyrolysis leads to the need of additional fuel. The integration of CLC requires the least due to its lowest energy penalty amongst the studied capture technologies.

CLC and CaL have the lowest levelized costs of CO_2 (LCOC), which are about 56$/t$CO_2$; while MEA-CA shows the highest, which is 83 $/t$CO_2$. As the reaction time increases, the LCOCs of all studied capture technologies decrease.

Taking into account the profit from carbon trading, CLC and MEA-CA show the highest and lowest net present value (NPV) and shortest and longest payback time (PBT) respectively, which are sensitive to the carbon price. At a carbon price of 70.1$/t$CO_2$, the PBT of CLC and MEA-CA are 3 years and 6 years.

CRediT authorship contribution statement

Yingying Sun: Software, Investigation, Validation, Writing – original draft, Writing – review & editing. **Beibei Dong:** Software, Validation, Investigation, Writing – original draft. **Liang Wang:** Investigation, Writing – original draft, Writing – review & editing, Supervision. **Hailong Li:** Conceptualization, Methodology, Writing – original draft, Writing – review & editing, Supervision, Funding acquisition. **Eva Thorin:** Writing – original draft, Writing – review & editing, Supervision.

Declaration of Competing Interest

The authors declare that they have no known competing financial interests or personal relationships that could have appeared to influence the work reported in this paper.

Acknowledgement

The authors gratefully acknowledge the financial support from National Natural Science Foundation of China (No. 51776140).

Appendix A. Supplementary data

Supplementary data to this article can be found online at https://doi.org/10.1016/j.enconman.2022.115835.

References

[1] National Aeronautics and Space Administration (NASA). Global Climate Change. https://climate.nasa.gov/.
[2] United Nations. The Paris Agreement. https://www.un.org/en/climatechange/paris-agreement.
[3] United Nations. Cut Global Emissions by 7.6 Percent Every Year for Next Decade to Meet 1.5°C Paris Target - UN Report, 2019. https://unfccc.int/news/cut-global-emissions-by-76-percent-every-year-for-next-decade-to-meet-15degc-paris-target-un-report.
[4] Anderson K, Peters G. The trouble with negative emissions. Science 2016;354:182–3.
[5] Edenhofer O. Climate change 2014: mitigation of climate change. Cambridge University Press; 2015.
[6] Giccs. Bioenergy and Carbon Capture and Storage. Bioenergy and Carbon Capture and Storage –. Global CCS Institute; 2019.
[7] Bioenergy International. Sweden's first bioenergy carbon capture and storage pilot inaugurated. https://bioenergyinternational.com/heat-power/swedens-first-bioenergy-carbon-capture-and-storage-pilot-inaugurated#:~:text=Swedish%20energy%20utility%20Stockholm%20Exergi%20AB%20has%20inaugurated,2019%2C%20by%20the%20Minister%20for%20Energy%20Anders%20Ygeman.
[8] Kemper J. Biomass and carbon dioxide capture and storage: A review. Int J Greenhouse Gas Control 2015;40:401–30.
[9] Kemper J., Biomass with carbon capture and storage (BECCS/Bio-CCS). IEA Greenhouse Gas R&D Program; 2017.
[10] Komandur J, Mohanty K. Fast pyrolysis of biomass and hydrodeoxygenation of bio-oil for the sustainable production of hydrocarbon biofuels. Hydrocarbon Biorefinery Elsevier 2022.:47–76.
[11] Chiong MC, Chong CT, Ng J-H, Lam SS, Tran M-V, Chong WWF, et al. Liquid biofuels production and emissions performance in gas turbines: A review. Energy Convers Manage 2018;173:640–58.
[12] Zhou X, Mahalingam S. Evaluation of reduced mechanism for modeling combustion of pyrolysis gas in wildland fire. Combust Sci Technol 2001;171:39–70.
[13] Moud PH, Kantarelis E, Andersson KJ, Engvall K. Biomass pyrolysis gas conditioning over an iron-based catalyst for mild deoxygenation and hydrogen production. Fuel 2018;211:149–58.
[14] Woolf D, Lehmann J, Lee DR. Optimal bioenergy power generation for climate change mitigation with or without carbon sequestration. Nat Commun 2016;7:1–11.
[15] Krull L. Meet Pyrolysis – the eco-friendly way to capture and store CO_2. The Brighter Side of News 2021. https://www.thebrighterside.news/post/meet-pyrolysis-the-eco-friendly-way-to-capture-and-store-co2#:~:text=%22The%20carbon%20capture%20occurs%20when,original%20biomass%20in%20the%20biocoal.
[16] Lim TC, Cuellar A, Langseth K, Waldon JL. Technoeconomic Analysis of Negative Emissions Bioenergy with Carbon Capture and Storage through Pyrolysis and Bioenergy District Heating Infrastructure. Environ Sci Technol 2022;56(3):1875–84.
[17] Schmidt H-P, Anca-Couce A, Hagemann N, Werner C, Gerten D, Lucht W, et al. Pyrogenic carbon capture and storage. GCB Bioenergy 2019;11(4):573–91.

[18] Cheng F, Small AA, Colosi LM. The levelized cost of negative CO_2 emissions from thermochemical conversion of biomass coupled with carbon capture and storage. Energy Convers Manage 2021;237:114115.

[19] Datta A, Hester T, Krishnamoorti R. Negative Emissions Technologies: Has Their Time Arrived? Forbes 2018. https://www.forbes.com/sites/uhenergy/2018/09/14/negative-emissions-technologies-has-their-time-arrived/?sh=7848f3df116c.

[20] Li H, Haugen G, Ditaranto M, Berstad D, Jordal K. Impacts of exhaust gas recirculation (EGR) on the natural gas combined cycle integrated with chemical absorption CO_2 capture technology. Energy Procedia 2011;4:1411–8.

[21] Kapetaki Z, Barbosa EM. Carbon Capture Utilisation and Storage Technology Development Report 2018 (CCUS). European Commission; 2019.

[22] H. Dieter, A. Bidwe, G. Scheffknecht. Pilot plant experience with calcium looping. Calcium and Chemical Looping Technology for Power Generation and Carbon Dioxide (CO_2) Capture. Elsevier2015. pp. 171-94.

[23] Lyngfelt A, Leckner B. A 1000 MWth boiler for chemical-looping combustion of solid fuels–Discussion of design and costs. Appl Energy 2015;157:475–87.

[24] H. Li, B. Dong, W. Nookuea, Q. Sun, E. Thorin, et al. Capturing CO_2 from bioenergy conversion – opportunities and challenges, manuscript.

[25] Bui M, Adjiman CS, Bardow A, Anthony EJ, Boston A, Brown S, et al. Carbon capture and storage (CCS): the way forward. Energy Environ Sci 2018;11(5):1062–176.

[26] Gardarsdottir SO, De Lena E, Romano M, Roussanaly S, Voldsund M, Pérez-Calvo J-F, et al. Comparison of technologies for CO_2 capture from cement production—Part 2: Cost analysis. Energies 2019;12:542.

[27] Ho MT, Bustamante A, Wiley DE. Comparison of CO_2 capture economics for iron and steel mills. Int J Greenhouse Gas Control 2013;19:145–59.

[28] Yang H, Fan S, Lang X, Wang Y, Nie J. Economic comparison of three gas separation technologies for CO_2 capture from power plant flue gas. Chin J Chem Eng 2011;19:615–20.

[29] Quader M, Ahmed S. Bioenergy with carbon capture and storage (BECCS): Future prospects of carbon-negative technologies. Clean Energy Sustain Development Elsevier 2017.:91–140.

[30] Lu Q, Li W-Z, Zhu X-F. Overview of fuel properties of biomass fast pyrolysis oils. Energy Convers Manage 2009;50:1376–83.

[31] Kan T, Strezov V, Evans TJ. Lignocellulosic biomass pyrolysis: A review of product properties and effects of pyrolysis parameters. Renew Sustain Energy Rev 2016;57:1126–40.

[32] Dhyani V, Bhaskar T. A comprehensive review on the pyrolysis of lignocellulosic biomass. Renewable Energy 2018;129:695–716.

[33] Cheng F, Luo H, Colosi LM. Slow pyrolysis as a platform for negative emissions technology: An integration of machine learning models, life cycle assessment, and economic analysis. Energy Convers Manage 2020;223:113258.

[34] Ranzi E, Cuoci A, Faravelli T, Frassoldati A, Migliavacca G, Pierucci S, et al. Chemical kinetics of biomass pyrolysis. Energy Fuels 2008;22:4292–300.

[35] Peters J.F., Iribarren D., Dufour J. Predictive pyrolysis process modelling in Aspen Plus. European Biomass Conference and Exhibition, Copenhagen, June 03-07, 2013.

[36] Sharma A, Mohanty B. Thermal degradation of mango (Mangifera indica) wood sawdust in a nitrogen environment: characterization, kinetics, reaction mechanism, and thermodynamic analysis. RSC Adv 2021;11:13396–408.

[37] Idriss I, Ahmed M, Grema A, Baba D. Modeling and Simulation of Pyrolysis Process for a Beech Wood Material. Arid Zone J Eng, Technol Environ 2017;13:710–7.

[38] Li K, Cousins A, Yu H, Feron P, Tade M, Luo W, et al. Systematic study of aqueous monoethanolamine-based CO_2 capture process: model development and process improvement. Energy Sci Eng 2016;4(1):23–39.

[39] Zhao R, Liu L, Zhao L, Deng S, Li S, Zhang Y. A comprehensive performance evaluation of temperature swing adsorption for post-combustion carbon dioxide capture. Renew Sustain Energy Rev 2019;114:109285.

[40] Hanak DP, Michalski S, Manovic V. From post-combustion carbon capture to sorption-enhanced hydrogen production: A state-of-the-art review of carbonate looping process feasibility. Energy Convers Manage 2018;177:428–52.

[41] Zhang S, He S, Gao N, Wang J, Duan Y, Quan C, et al. Hydrogen production from autothermal CO_2 gasification of cellulose in a fixed-bed reactor: Influence of thermal compensation from CaO carbonation. Int J Hydrogen Energy 2022.

[42] Gao N, Śliz M, Quan C, Bieniek A, Magdziarz A. Biomass CO_2 gasification with CaO looping for syngas production in a fixed-bed reactor. Renewable Energy 2021;167:652–61.

[43] Rolfe A, Huang Y, Haaf M, Rezvani S, McIlveen-Wright D, Hewitt N. Integration of the calcium carbonate looping process into an existing pulverized coal-fired power plant for CO_2 capture: Techno-economic and environmental evaluation. Appl Energy 2018;222:169–79.

[44] Khan MN, Cloete S, Amini S. Efficiency improvement of chemical looping combustion combined cycle power plants. Energy Technology 2019;7:1900567.

[45] Ephraim A, Minh DP, Lebonnois D, Peregrina C, Sharrock P, Nzihou A. Co-pyrolysis of wood and plastics: influence of plastic type and content on product yield, gas composition and quality. Fuel 2018;231:110–7.

[46] Shahbaz M, AlNouss A, Parthasarathy P, Abdelaal AH, Mackey H, McKay G, et al. Investigation of biomass components on the slow pyrolysis products yield using Aspen Plus for techno-economic analysis. Biomass Convers Biorefin 2022;12(3):669–81.

[47] Visconti A, Miccio M, Juchelková D. An Aspen Plus tool for simulation of lignocellulosic biomass pyrolysis via equilibrium and ranking of the main process variables. Int J Mathemat Model Method Appl Sci 2015;9:71–86.

[48] Merel J, Clausse M, Meunier F. Experimental investigation on CO_2 post–combustion capture by indirect thermal swing adsorption using 13X and 5A zeolites. Ind Eng Chem Res 2008;47:209–15.

[49] Vorrias I, Atsonios K, Nikolopoulos A, Nikolopoulos N, Grammelis P, Kakaras E. Calcium looping for CO_2 capture from a lignite fired power plant. Fuel 2013;113:826–36.

[50] Ortiz C, Chacartegui R, Valverde J, Becerra J. A new integration model of the calcium looping technology into coal fired power plants for CO_2 capture. Appl Energy 2016;169:408–20.

[51] Arias B, Diego ME, Abanades JC, Lorenzo M, Diaz L, Martínez D, et al. Demonstration of steady state CO2 capture in a 1.7MWth calcium looping pilot. Int J Greenhouse Gas Control 2013;18:237–45.

[52] Preem. Sweden's first pyrolysis oil plant for biofuels under construction., https://news.cision.com/preem-ab/r/sweden-s-first-pyrolysis-oil-plant-for-biofuels-under-construction,c3136758; 2020.

[53] Şensöz S, Can M. Pyrolysis of pine (Pinus brutia Ten.) chips: 1. Effect of pyrolysis temperature and heating rate on the product yields. Energy Sources 2002;24:347–55.

[54] Bridgwater AV. Review of fast pyrolysis of biomass and product upgrading. Biomass Bioenergy 2012;38:68–94.

[55] Dahawi YA, Abdulrazik A, Seman MNA, Aziz MAA, Yunus MYM. Aspen Plus Simulation of Bio-Char Production from a Biomass-Based Slow Pyrolysis Process. Key Engineering Materials Trans Tech Publ 2019:336–41.

[56] Şensöz S. Slow pyrolysis of wood barks from Pinus brutia Ten. and product compositions. Bioresour Technol 2003;89:307–11.

[57] Ali U, Agbonghae EO, Hughes KJ, Ingham DB, Ma L, Pourkashanian M. Techno-economic process design of a commercial-scale amine-based CO_2 capture system for natural gas combined cycle power plant with exhaust gas recirculation. Appl Therm Eng 2016;103:747–58.

[58] Peters MS, Timmerhaus KD, West RE. Plant design and economics for chemical engineers. McGraw-Hill New York; 2003.

[59] Cepci. Chemical engineering plant cost index (CEPCI). New York: Access Intelligence LLC.; 2021.

[60] Cormos C-C. Economic evaluations of coal-based combustion and gasification power plants with post-combustion CO_2 capture using calcium looping cycle. Energy 2014;78:665–73.

[61] EU ETS. https://ec.europa.eu/clima/eu-action/eu-emissions-trading-system-eu-ets_en.